



Effect of cobalt substitution on microstructure and magnetic properties in ZnO nanoparticles

Chandana Rath^{1*}, Sonal Singh¹, P Mallick², D Pandey¹, N P Lalla³ and N C Mishra⁴

¹School of Materials Science & Technology, Institute of Technology, Banaras Hindu University, Varanasi-221 005, Uttar Pradesh, India

²Department of Physics, North Orissa University, Baripada-757 003, Orissa, India

³UGC-DAE Consortium for Scientific Research, Khandwa Road, Indore-452 017, Madhya Pradesh, India

⁴Department of Physics, Utkal University, Bhubaneswar-751 004, Orissa, India

E-mail : chandanarath@yahoo. com

Abstract : Ferromagnetic semiconductors have been actively pursued because of their potential as spin polarized carrier sources and easy integration into semiconductor technology. One such material, ZnO has been shown to be a potential Diluted Magnetic Semiconductor (DMS). The appearance of ferromagnetism, however, is found to be sensitive to the processing conditions. We report synthesis of ZnO nanoparticles of size ~20 nm by a simple co-precipitation technique using metal nitrates and NaOH as precipitant. The particles are self-organised and reveal single crystalline behaviour in electron diffraction pattern. Incorporation of Co in ZnO matrix leads not only to the reduction in crystallite size but also to the modification of the structure. At 5% Co, the particles are highly textured. The particles also aggregate and the aggregated mass have nearly rectangular shape as seen through TEM. Increasing Co to 10%, results into further reduction of particle size and the particles self organize in a line, which looks like nanofibers. This alignment of particles increases by increasing the Co content further. This type of growth of nanofibers above Co \geq 10% is well correlated with the anisotropic peak broadening observed in the XRD spectra. In addition, Co substitute Zn site up to 20% without showing any extra phase in XRD spectra as compared to 7 to 10% in case of bulk. Transport and magnetic studies indicate that conductivity increases with increasing Co content, but carrier mediated ferromagnetism is absent down to 10 K.

Keywords : Dilute magnetic semiconductor, nanoparticles, susceptibility, ZnO

PACS Nos. : 91.60.Ed, 61.46.+w, 75.50.Tt, 75.75.+a, 73.61.Ga

1. Introduction

Ferromagnetic semiconductors have been actively pursued because of their potential as spin polarized carrier sources and easy integration into semiconductor technology. Theoretical developments [1,2] have shown that wide band gap semiconductors are the most promising candidates for achieving room temperature ferromagnetism. Zinc Oxide, a wide band gap (3.37 eV) *n*-type piezoelectric semiconductor with large exciton

*Corresponding Author

binding energy, is an important electronic and photonic material [3]. It is also used as a host material for the growth of diluted magnetic semiconductor.

A large number of studies have been carried out on polycrystalline bulk transition metal doped ZnO semiconductor synthesized by ceramic route at various temperatures [4,5] and thin films grown by Pulsed Laser Deposition, Molecular Beam Epitaxy, RF sputtering, Sol-gel technique [6–9]. The observed bulk ferromagnetism is ascribed mainly to non-optimal synthesis conditions leading to formation of second phases, which contradict the existing theory. We report here the preparation of single phase Co doped ZnO by a simple co-precipitation route and examine the origin and intrinsic nature of ferromagnetism in these systems.

2. Experimental

The compounds with nominal composition $\text{Zn}_{1-x}\text{Co}_x\text{O}$ ($x = 0, 0.01, 0.025, 0.05, 0.1, 0.15, 0.2, 0.25$) are synthesized by co-precipitation method using metal nitrate solutions and NaOH as precipitant. The obtained materials are crushed into fine particles and are analyzed for their composition, microstructure, transport and magnetic properties. X-Ray diffraction (Rigaku Powder Diffractometer), Scanning Electron Microscopy (Model : JEOL JSM 5600 Resolution : 3.5 nm) and Transmission Electron Microscopy (Model : Tecnai 20 G2) are used for the phase and microstructural studies. DC two probe resistivity measurement set-up is used to measure the resistivity in the temperature range 80–300 K. Magnetic measurements are carried out by Physical Properties Measurement System (PPMS).

3. Results and discussion

X-Ray diffraction pattern of the as-synthesized samples obtained without and with Co doping at various concentrations are shown in Figure 1.

Bhat *et al* [10] have shown the presence of ZnCo_2O_4 and Co_3O_4 for $x > 0.07$ in $\text{Zn}_{1-x}\text{Co}_x\text{O}$ prepared from acetates. To better understand the origin of magnetism Zhang *et al* prepared polycrystalline bulk form and have shown pure phase of $\text{Zn}_{1-x}\text{Co}_x\text{O}$ for x up to 0.1 [11]. Yeng *et al* followed hydrothermal synthesis method using nitrates and KOH solvent and observed formation of $\text{Co}(\text{OH})_2$ at $x = 9.9$ as second phase [12]. Other reports have indicated that Co can be incorporated in the matrix of ZnO up to 7–10 at % without forming any second phase [13,14]. All these reports thus indicate that Co has a limited solubility in ZnO up to 10 at%. In contrast to this, we observe that all the peaks match well with the Wurtzite structure of ZnO in both pure and Co doped ZnO samples up to a cobalt concentration of 20%. The solubility limit of Co in ZnO is thus enhanced through co-precipitation technique compared to all earlier reports. The extra small XRD peak indicated by * in the Figure 1 corresponds to the impurity phase observed in 20 and 25% Co doped samples. The XRD peaks show broadening with increase in Co incorporation, which may be due to the decrease of

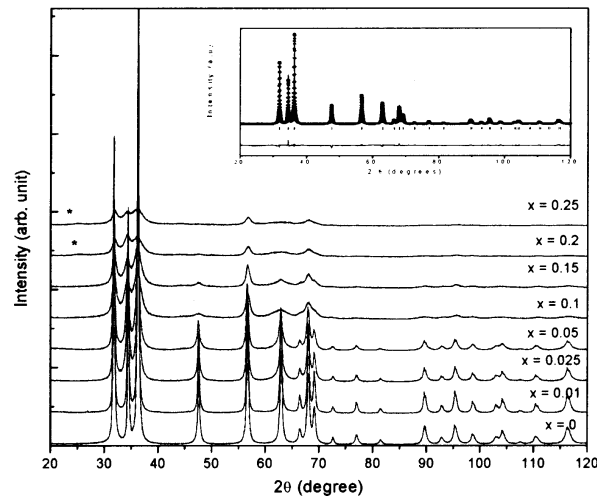


Figure 1. XRD of $\text{Zn}_{1-x}\text{Co}_x\text{O}$ (* denotes the impurity phase). Inset shows observed (dots), calculated (continuous line), and difference (bottom line) powder diffraction profiles of ZnO obtained from full pattern Reitveld analysis in the range 20 to 120 degrees using P6₃MC space group. The tick marks above the difference plot show the positions of the Bragg peaks.

crystallite size. The crystallite size is estimated from XRD line width of (101) peak using Scherrer formula after Lorentzian fitting of the profile. The crystallite size is found to decrease with increase Co concentration. Inset shows a typical Rietveld fit for pure ZnO using Fullprof program with P6₃mc space group. A good fit between observed and calculated profiles are obtained for pure sample which can be seen from the flat difference profile. The unit cell volume calculated from fitting and found to be increasing with increase in Co concentration (Table 1). This indicates that Zn^{2+} in tetrahedral coordination (0.60 Å) is not replaced by Co^{2+} (0.58 Å) in tetrahedral coordination but by divalent octahedral Co whose ionic radius is in between 0.65 Å (low spin) and 0.745 Å (high spin) [13].

Table 1. Estimation of crystallite size after Lorentzian fitting of the profile and lattice parameter after Reitveld fitting.

Sample	d_{101} (nm)	Lattice volume (nm) ³
ZnO	31.00	47.596
$\text{Zn}_{0.99}\text{Co}_{0.01}\text{O}$	30.40	47.596
$\text{Zn}_{0.975}\text{Co}_{0.025}\text{O}$	24.00	47.605
$\text{Zn}_{0.95}\text{Co}_{0.05}\text{O}$	17.50	47.654
$\text{Zn}_{0.9}\text{Co}_{0.1}\text{O}$	6.41	47.802
$\text{Zn}_{0.85}\text{Co}_{0.15}\text{O}$	6.30	47.868

The TEM picture of pure ZnO (Figure 2a) reveals that the size of nanoparticles is within 20 to 30 nm, which matches well with the crystallite size calculated from XRD linewidth (Table 1). The enlarged view further shows that tiny particles are self-organized

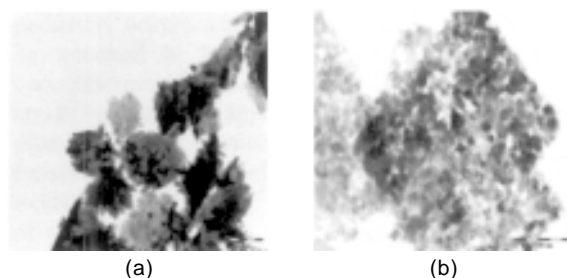


Figure 2. (a) Transmission Electron Micrograph of pure ZnO (left) and (b) enlarged view (right).

(Figure 2b). The selected area electron diffraction (SAED) pattern reveals self-organization of nanoparticles and single crystalline behaviour where all nanoparticles diffract in hexagonal pattern. Each spot in the SAED pattern is indexed, which matches well with the d -spacing of Wurtzite ZnO. The particles are textured and are oriented from one another by 5 to 6 degrees. On tilting, the self organized aggregates show [110] zone patterns (Inset of Figure 3).

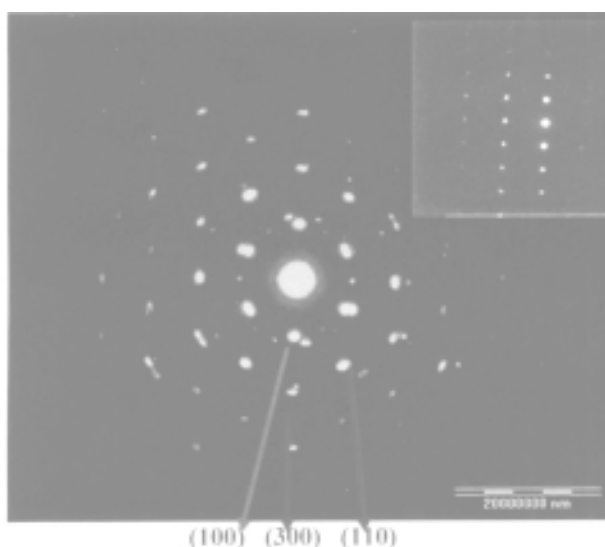


Figure 3. Electron diffraction pattern of pure ZnO and inset is the ED pattern after tilting the camera.

As Co concentration increases to 5 at%, TEM shows well defined rectangular shape patches with few star shaped nanorods (Figure 4a). A closure view of one patch is shown in Figure 4b showing the reduction in particle size compared to the pure ZnO. The electron diffraction pattern of the same is shown as inset in Figure 4b, which indicates that the particles are highly textured and single crystalline. At 10% Co concentration and above, well defined nanofibers are observed in both SEM and TEM micrographs (Figures 5a and 5b). TEM also confirms that the particle size reduces with increasing Co concentration as observed from XRD linewidth analysis. Detail TEM analysis undertaken by acquiring TEM image by tilting the camera at different angles.

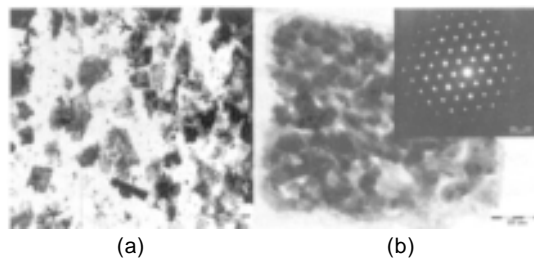


Figure 4. (a) TEM of ZnO doped with 5% Co (left) and (b) SAED pattern of one square shape patch, inset is the electron diffraction (right).

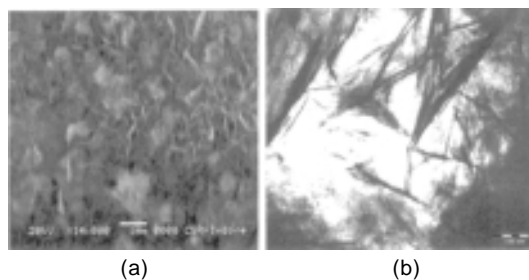


Figure 5. Typical SEM (a) and TEM (b) picture of 5% Co doped ZnO shown in left and right respectively.

It was observed that fine particles align themselves in a line and looks like nanofibers and the alignment is different in other angles. This type of growth of nanofibers above $\text{Co} \geq 10\%$ is well correlated with the anisotropic peak broadening observed in the XRD spectra (Figure 1). The alignment of fine particles in a line, which looks like a nanofiber, increases with increase in Co concentration. The SAED pattern of these nanofibers shows polycrystalline behaviour. No impurity phases corresponding to Co metal, CoO, Co_3O_4 were detected from SAED pattern upto $\text{Co} \leq 15\%$.

Resistivity measurement shows the semiconducting behaviour in all Co doped ZnO samples after heating 500°C for 4 hours (Figure 6). The room temperature value of the resistivity is found to be reduced by an order of magnitude in 5% Co and 4 orders of magnitude in 25% Co as compared to 1% Co doped sample. Fitzgerald *et al* [14] have observed enhancement of resistivity and reduction in magnetic moment with increase in Co concentration in thin films of Co doped ZnO. However, in the present case the orders of magnitude reduction in resistivity occurs with increase in Co content. This can be assumed to be due to enhancement of carrier concentration. Presence of free carriers is a necessary condition for the appearance of ferromagnetism in dilute magnetic semiconductor. Free carriers can be induced by doping, defects or by Co ions in another oxidation state like Co^{3+} . In the present case the absence of second phase rules out the presence of Co^{3+} . The enhancement of charge carriers with Co doping could be due to the oxygen vacancy. Thus, we may expect ferromagnetism in these samples, which will be due to the increase in carrier concentration with Co content.

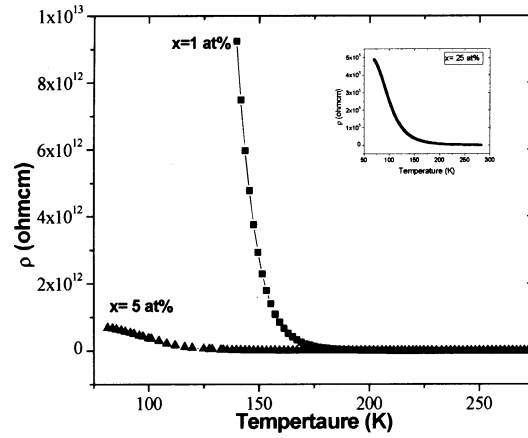


Figure 6. Resistivity vs. temperature for $\text{Zn}_{1-x}\text{Co}_x\text{O}$ ($x = 0.01$ and 0.05) and $x = 0.25$ sample is shown in inset.

Figure 7 represents the dependence of inverse molar susceptibility ($1/\chi$) on temperature (T) for the samples with $x = 0.05$ and 0.1 . It is clearly observed that samples show paramagnetic behaviour following Curie-Weiss law, which is consistent with the reported data [15]. The θ values, obtained by extrapolation of fit in the linear part of the curves up to an intersection with T axis, were all negative. This indicates that magnetic ions in the lattice are coupled antiferromagnetically (AFM). The magnetization data are acquired upon warming from 2 to 300 K in an external field of

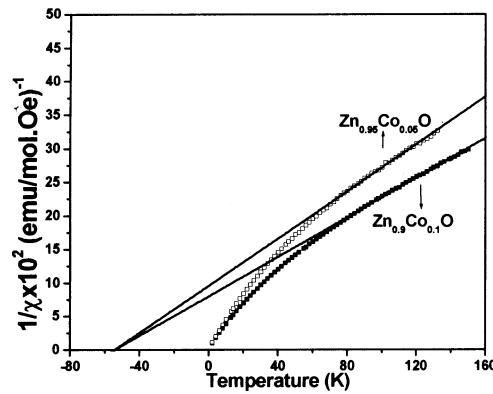


Figure 7. $1/\chi$ vs. T of $\text{Zn}_{1-x}\text{Co}_x\text{O}$ ($x = 0.1$ and 0.05) samples. Solid lines corresponding to the Curie-Weiss fittings extrapolated up to the intersection with T axis.

500 Oe after zero field cooling (ZFC) and FC displayed identical behaviour. Temperature dependence of susceptibility for $\text{Co} = 0.1$ and $\text{Co} = 0.05$ samples are fitted with $J = 1.4$ which gives an effective magnetic moment (μ_{eff}) $\sim 3.66 \mu_B$. This moment is matched well with Co^{2+} high spin state which shows a calculated μ_{eff} having spin magnetic moment only equal to $3.87 \mu_B$. Magnetization vs. field at 10 K does not show any hysteresis loop. Though the carrier concentration is enhanced by Co incorporation, the

absence of ferromagnetism rules out the carrier mediated ferromagnetism in these samples.

4. Conclusions

A simple co-precipitation technique is used to prepare single phase Co doped ZnO nanoparticles. A high solubility limit of Co substitution in the place of Zn has been achieved in these nanoparticles as compared to the earlier reported literatures. Even with high solubility limit of Co, plots of magnetization with temperature and magnetic field with temperature show paramagnetic behaviour down to 10 K. This confirms that ZnO is not a suitable DMS material.

Acknowledgment

We acknowledge UGC-DAE-CSR, Indore for magnetic characterizations.

References

- [1] T Dielt, H Ohno, F Matsukura, J Cibert and D Ferand *Science* **287** 1019 (2000)
- [2] K Sato and H Katayama-Yoshida *Semicond. Sci. Technol.* **17** 367 (2002)
- [3] M H Huang, S Mao, H N Feick, H Q Yan, Y Y Wu, H Kind, E Weber, R Russo and P D Yang *Science* **292** 1897 (2001)
- [4] S Kolesnik, B Dabrowski and J Mais *J. Appl. Phys.* **95** 2582 (2004)
- [5] J Zhang, R Skomski and D J Sellmyer *J. Appl. Phys.* **97** 10D303 (2005)
- [6] K Ueda, H Tabat and T Kawai *Appl. Phys. Lett.* **79** 988 (2001)
- [7] Z Jin, T Fukumura, M Kawasaki, K Ando, H Saito, T Sekiguchi, Y Z Yoo, M Murakami, Y Matsumoto, T Hasegawa and H Koinuma *Appl. Phys. Lett.* **78** 3824 (2001)
- [8] A Dinia, J P Ayoub, G Schmerber, E Beaurepaire, D Muller and J J Grob *Phys. Lett.* **A333** 152 (2004)
- [9] C Liu, F Yun, B Xiao, S J Cho, Y T Moon and H Morkoc, M Abouzaid, R Ruterana, K M Yu and W Walukiewicz *J. Appl. Phys.* **97** 126107 (2005)
- [10] S V Bhat and F L Deepak *Solid State Commun* **135** 345 (2005)
- [11] Y B Zhang, S Li, T T Tan and H S Park *Solid State Commun* **137** 142 (2006)
- [12] L W Yeng, X L Wu, T Qui, G G Siu and P K Chu *J. Appl. Phys.* **99** 074303 (2006)
- [13] M Bouloudenine, N Viart, S Colis, J Kortus and A Dinia *Appl. Phys. Lett.* **87** 052501 (2005)
- [14] C B Fitzgerald, M Venkatesan, J G Lunney, L S Dorneles and J M D Coey *Appl. Surface Sci.* **247** 493 (2005)
- [15] B A Hunter *IUCC Powder Diffraction* **20** p21 (1998)